Article

Analyzing the Genetic Variation and Geographic Distribution Patterns of *Xanthomonas citri* pv. *citri* Strains: Significance for Developing Sustainable Control Methods in Citrus Production in Burkina Faso

Kevin Ben Fabrice Zerbo *, Florence Yameogo , Issa Wonni , Irénée Somda

Posted Date: 8 April 2024

doi: 10.20944/preprints202404.0465.v1

Keywords: Citrus; Xanthomonas citri pv. citri; TAL effectors; Type 3 effectors; Burkina Faso

Preprints.org (www.preprints.org) | NOT PEER-REVIEWED | Posted: 8 April 2024 doi:10.20944/preprints202404.0465.v1

Article

Analyzing the Genetic Variation and Geographic Distribution Patterns of *Xanthomonas citri* pv. *citri* Strains: Significance for Developing Sustainable Control Methods in Citrus Production in Burkina Faso

Kevin Ben Fabrice Zerbo [1,2,*], Florence Yameogo [1,2], Issa Wonni [1] and Irénée Somda [2]

[1] Centre National de la Recherche Scientifique et Technologique/Institut de l'Environnement et de Recherches Agricoles (INERA)/ Laboratoire Mixte International/ Observatoire des agents pathogènes, Biosécurité et Biodiversité (LMI PathoBios); 01 BP 910. Bobo Dioulasso, Burkina Faso; yamflore31@yahoo.fr (F.Y); wonniissa@yahoo.fr (I.W)

[2] Université Nazi BONI/Clinique des Plantes; 01 BP1091. Bobo Dioulasso, Burkina Faso; ireneesomda@yahoo.fr (I.S)

* Correspondence: benzerbo@yahoo.fr, 226 74767132

Abstract: It is essential to have a thorough knowledge of the genetic variation among different strains of *Xanthomonas citri* pv. *citri* (*Xcc*), which is responsible for causing citrus bacterial canker. This understanding is important for studying the disease's characteristics, population structure, and evolution, and ultimately for developing sustainable methods of control. A total of 48 strains, obtained from citrus production areas in Burkina Faso in 2012, 2020, and 2021, were subjected to polymerase chain reaction (PCR) tests using specific primers. The aim was to examine the distribution of type 3 effectors (T3E) and determine the geographical origins of the strains. The examination of the distribution of type 3 non-transcription activate like effectors (TALE) indicates a broader range in strains obtained in 2020 and 2021 compared to those obtained in 2012. However, all strains possess a shared set of three genes, specifically XopE2, XopN, and AvrBs2. Furthermore, all examined effectors were observed in the Bobo-Dioulasso region. Regarding the characterization of TALEs, two profiles containing two to three TALEs were discovered. Profile 1, consisting of two TALEs, was found in 37 *Xcc* strains, whereas Profile 2, comprising three TALEs, was detected in 11 strains. Out of the three TALEs (A, B, and C) that were identified, TALEs B and C were present in all strains. The correlation matrix indicated a positive association between the T3E content of strains and the duration of their isolation. Principal component analysis revealed a limited organization of the strains under investigation

Keywords: citrus; *Xanthomonas citri* pv. *citri*; TAL effectors; type 3 effectors; Burkina Faso

---

1. Introduction

Citrus Bacterial Canker (CBC), caused by *Xanthomonas citri* pv. *citri* (Xcc), is a major bacterial disease that has severe economic consequences in citrus-growing regions that have a tropical or subtropical climate [1,2]. The intensity of symptoms varies geographically, which might lead to decreased productivity and limitations on exports. The pathogen was recently documented in Burkina Faso by [3]. Further investigation conducted by [4] revealed widespread instances of bacterial canker in nurseries and production regions, with occurrence rates ranging from 50% to 90%. As a result, fruit output losses per hectare due to CBC varied from 18.45% to 90.8%, depending on the species.

The *Xcc* strain has been the subject of many epidemiological and population structure research due to its economic importance, regulatory consequences, and worldwide spread [5,6]. In the last ten years, collaborative research from around the world has helped to clarify the worldwide genetic variation of *Xcc* [7,8]. The basis of *Xcc* strain characterization is centered around the type 3 secretion system (T3SS) and its associated proteins, including the type 3 effectors (T3E), which are secreted during interactions with plant cells. Every Xanthomonas strain has the ability to generate at least 15 distinct Type III Effector proteins (T3Es) [9]. A total of 26 T3Es have been found in *Xcc* using bioinformatics research [10]. It is worth mentioning that within Xanthomonas T3Es, there is a particular group called TAL (Transcription Activator-Like) effectors. These effectors function as transcription factors and are transported to the nucleus. Once in the nucleus, they control the expression of host genes in a way that benefits the pathogen. This information is supported by references [11,12]. Strains of the Xanthomonas genus exhibit variation in the quantity of TALEs.

Although there is a wealth of material available on the worldwide genetic makeup of *Xcc* groups, there is a scarcity of studies specifically focused on Burkina Faso. Remarkably, a solitary study has investigated the genetic correlations between strains originating from Burkina Faso and Mali.

The objective of this study is to examine the occurrence of T3Es (Type III Effector Proteins) and TALEs (Transcription Activator-Like Effectors) in *Xcc* strains that were obtained in 2012, 2020, and 2021 from various citrus production locations in Burkina Faso. In addition, the study aims to examine the relationship between the content of T3Es in *Xcc* strains, their geographic origins, and the years in which they were isolated.

2. Materials and Methods

2.1. Collection Site

The study was conducted in four provinces located within three administrative zones of Burkina Faso, which serve as the primary fruit production regions. The provinces of Bazega, Houet, Kénédougou, and Ziro were present. A total of eleven (11) citrus production sites were examined. The production sites in Houet included Kodéni, Bobo Dioulasso, Badara, and Tanwogoma. In Kénédougou, there were the Orodara, Koloko, and Gnadia sites. The Lou site was located in Ziro, and in Bazega, there were the Lilbouré, Timboué, and Dayasmnere sites (Figure 1). These sites are located within two specific agro-ecological zones in Burkina Faso. The two main zones in Sudan are the northern Sudanian zone, which receives an annual rainfall ranging from 700 to 900 mm, and the southern Sudanian zone, which receives an annual rainfall ranging from 900 to 1200 mm.

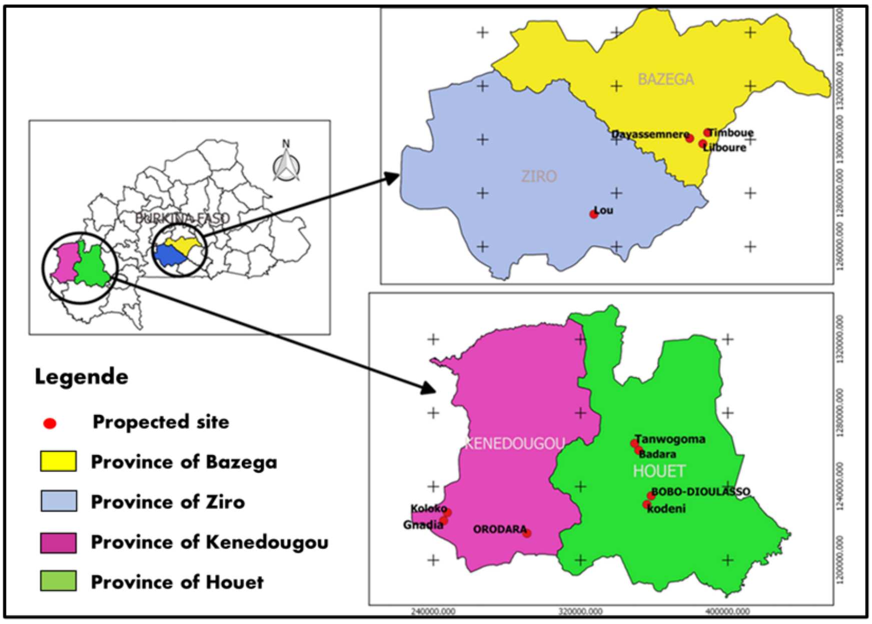

Figure 1. Geographic coordinates of the *Xcc* strains utilized in this investigation.

2.2. Material

The study concentrated on *Xcc* strains obtained from samples gathered from the primary citrus production areas in Burkina Faso. The samples were obtained from all the citrus species that harbored *Xcc* and were collected at the sites. In 2012, the Phytopathology/Bacteriology Laboratory team at the Institute for the Environment and Agricultural Research (INERA) Farakoba conducted surveys and isolations. We utilized 31 *Xcc* strains obtained from their collection for our study. Furthermore, our study contributed to the enrichment of this collection by including *Xcc* strains that were isolated. Table (1) displays the attributes of the 2012 *Xcc* strains that were utilized.

Table 1. Characteristics of strains used**.**

Strain code	Hosts plants	Province	Site	Year of collection
864	*C. reticulata* × *C. paradisi*	Kénédougou	Orodara	2012
865	*C. reticulata* × *C. paradisi*	Kénédougou	Orodara	2012
866	*C. reticulata* × *C. paradisi*	Kénédougou	Orodara	2012
867	*C. reticulata* × *C. paradisi*	Kénédougou	Orodara	2012
868	*C. reticulata* × *C. paradisi*	Kénédougou	Orodara	2012
869	*C. reticulata* × *C. paradisi*	Kénédougou	Orodara	2012
870	*C. reticulata* × *C. paradisi*	Kénédougou	Orodara	2012
871	*C. reticulata* × *C. paradisi*	Kénédougou	Orodara	2012
872	*C. reticulata* × *C. paradisi*	Kénédougou	Orodara	2012
873	*C. reticulata* × *C. paradisi*	Kénédougou	Orodara	2012
879	*C. clementina*	Kénédougou	Orodara	2012
880	*C. clementina*	Kénédougou	Orodara	2012
881	*C. clementina*	Kénédougou	Orodara	2012
882	*C. sinensis*	Kénédougou	Orodara	2012
883	*C. sinensis*	Kénédougou	Orodara	2012
884	*C. sinensis*	Kénédougou	Orodara	2012
885	*C. sinensis*	Kénédougou	Orodara	2012
886	*C. reticulata*	Kénédougou	Orodara	2012
890	*C. volkameriana*	Kénédougou	Orodara	2012
891	*C. volkameriana*	Kénédougou	Orodara	2012
895	*C. volkameriana*	Kénédougou	Orodara	2012
896	*C. volkameriana*	Kénédougou	Orodara	2012
897	*C. volkameriana*	Kénédougou	Orodara	2012
887	*C. sinensis*	Houet	Tangoma	2012
876	*C. reticulata* × *C. paradisi*	Houet	Badala	2012
888	*C. sinensis*	Houet	Gnadga	2012
889	*C. reticulata* × *C. paradisi*	Kénédougou	Koloko	2012
874	*C. reticulata* × *C. paradisi*	Kénédougou	Koloko	2012
875	*C. reticulata* × *C. paradisi*	Kénédougou	Koloko	2012
877	*C. sinensis*	Kénédougou	Koloko	2012
878	*C. sinensis*	Kénédougou	Koloko	2012

2.3. Methods

2.3.1. Isolation

The isolation procedure consisted of gathering pieces from organ tissues exhibiting symptoms, which included both diseased and unaffected sections. The pieces were subjected to consecutive disinfection procedures using ethanol (70%), bleach (0.1%), and then rinsed with sterile distilled water. Subsequently, the fragments were pulverized and then mixed with 1 cc of sterile distilled water. The suspension was permitted to remain undisturbed for at least 30 minutes at ambient temperature, with periodic agitation to enhance bacterial dispersion. Next, a 50 µl portion of the suspension was uniformly distributed over Yeast Peptone Glucose Agar (LPGA) nutrient medium, which was enhanced with antibiotics including kasugamycin (20 mg/l), cephalexin (40 mg/l), and propiconazole (fungicide at 40 mg/l).

The incubation period lasted for 72 to 96 hours. During this time, bacterial colonies with morphological traits similar to the reference strain, specifically ivory-white color, were chosen and purified for pathogenicity tests.

2.3.2. Pathogenicity Testing

In order to evaluate the ability of *Xcc* strains to cause disease, citrus plants grown under semi-controlled conditions were used. The leaves were infected by infiltrating them with a bacterial solution containing 108 bacteria per milliliter, which corresponds to an optical density (OD) of 0.2 at a wavelength of 600 nm. The optical density (OD) was measured by transferring 1 ml of the bacterial suspension into a spectrophotometer cuvette. The spectrophotometer was calibrated at 0.2 with an error of 10%. The measurement was determined using the following formula:

$$\text{Volume of sterile distilled water to be added} = \frac{\textbf{OD obtained} - \textbf{OD required}}{\textbf{OD required x Vr}}$$

Vr = Volume of bacterial suspension remaining after sampling 1 ml to measure OD.

A citrus plant was treated with sterile distilled water as a control. The plants that were given a vaccine were placed in an environment that closely resembles their natural habitat, with temperatures ranging from 28 to 30 degrees Celsius and an average relative humidity of 75%. Visual symptoms were detected starting from 7 days post-inoculation.

2.3.3. Identification of Xcc Strains

For the identification of *Xcc* strains, specific primers were used in PCR amplification. The primer sequences were REP_FW ATG-TCC-GAC-ATG-AAA-GTT-AAT-T and REP_RV CGC-TTC-TCC-TGC-ATT. The PCR reaction mixture, with a volume of 25 µl per reaction, comprised 1X PCR buffer colored with 5X at 3 mM MgCl2 (25 mM), 1 µM REP_FW primer (10 µM), 1 µM REP_RV primer (10 µM), 0.2 mM of each deoxynucleotide triphosphate (dNTP) (2.5 mM), 0.25 U (5 U/µl) of Taq DNA polymerase and 2.5 µl of DNA sample at 20 ng/µl. The PCR program involved an initial denaturation phase at 95 ºC for 2 min, followed by 35 cycles at 95 ºC for 60 sec, 58 ºC for 70 sec, and 72 ºC for 75 sec, concluding with a final elongation phase at 72 ºC for 10 min. The resulting amplification products, expected to be 222 bp in size, were analyzed on a 2% agarose gel in 0.5X Tris- Borate-EDTA (TBE) buffer after staining with Ethidium Bromide (BET).

2.3.4. Analysis of Type 3 Effectors

Out of all the isolated *Xcc* strains, 11 T3E genes with high levels of variation were identified, as stated in reference [14] and shown in Table 2. The DNA extracted using the Promega Kit was subjected to PCR amplification. The reaction mixture contained 20 ul and consisted of 1X Go Taq Buffer (Promega), 200 mM dNTP, 0.5 µM of each primer, 0.4 U Go Taq Polymerase (final concentrations), and 1 µl of DNA (20 ng/µl).

The amplification conditions employing T3E primers consisted of an initial denaturation phase lasting 2 minutes at a temperature of 94 °C. This was followed by 30 reaction cycles, each including denaturation at 94 °C for 1 minute, hybridization at 60 °C for 1 minute, elongation at 72 °C for 2 minutes, and a final extension of 10 minutes at 72 °C [14]. The amplicons obtained were separated using 1% agarose gel electrophoresis, which included 2% BET, in a 0.5X TAE buffer (Tris Acetate 50 mM, 1 mM). The separation process was carried out at 100 Volts for a duration of 40 minutes.

Table 2. List of T3Es used in this study.

Oligo name	Sequence	Th °C	Size (bp)
xopB-F	ATG-AAG-GCA-GAG-CTC-ACA-CGA	49,2	1835
xopB-R	TCA-GGC-GCG-GGT-TGG-TGC-GAA-GTA	57,4	
xopD-F	ATG-GAA-TAT-ATA-CCA-AGA-ATG-AAG-C	46	1638
xopD-R	CTA-GAA-CTT-TTT-CCA-CCA-CTT-GC	48,4	
xopE2-F	ATG-GGG-CTA-TGC-AGT-TCA-AAG-C	49,7	393
xopE2-R	TCA-CCA-ACT-CAA-GGG-TGG-GC	64	
xopO-F	ATG-ATC-AAC-ACT-TCC-GTC-AAG	45,3	636
xopO-R	TCA-CCT-GTT-TAT-CCG-ACG-AC	60	
xopN-F	ATG-AAG-TCA-TCC-GCA-TCC-GTC	49,2	2090
xopN-R	GTG-CAG-TTC-CGT-CCC-CAA-GTT-CC	55,5	
xopQ-F	ATG-CAG-CCC-ACC-GCA-ATC	58	1124
xopQ-R	TCA-GCG-CCC-GCG-TTG-CC	60	
xopX-F	ATG-GAG-ATC-AAG-AAA-CAG-CAA-ACC	48,9	1864
xopX-R	TCA-GGA-CGA-AGG-CAC-AGT-GC	64	
avrBs2-F	GGA-CTA-GTC-CTG-CCG-GTG-TTG-ATG-CAC-GA	60,7	2118
avrBs2-R	CCG-CTC-GAG-CGG-TGA-TCG-GTC-AAC-AGG-CTT-TC	64,4	
avrBs1-F	ATG-TCC-GAC-ATG-AAA-GTT-AAT-T	42,3	1338
avrBs1-R	TTA-CGC-TTC-TCC-TGC-ATT-TG	58	
avrXccA1-F	ATG-CCC-AAC-GCA-TCG-CCT-GCA	53,1	813
avrXccA1-R	CGC-AGG-TCT-GCA-CCG-AAC-TCA-G	55,3	
avrXccA2-F	GTG-CTG-GAG-AGT-GCC-G	54	1442
avrXccA2-R	TCA-TCG-GCA-GGG-TTG-TGG	58	

Note: Th: Hybridization temperature; bp: Base pair.

2.3.5. Amplification of TAL Effectors

The primers REP_FW (GAGTTGAGAGGTCCACCGTTAC) and REP_RV (GGGAAGACGGCGATTGGTTC) described by [8] were used to amplify the TAL effectors of Xcc strains. They are positioned in the conserved regions of the TALEs close to the repeats. PCR assays were performed using 50 µl of reaction mixture containing 1 µl of DNA at 20 ng/µl, 10 µl of 5X Buffer, 1 µl of dNTPs (10 mM), 0.5µl of betaine (100 mM), 0.32 µl of 10X GO Taq buffer (Promega) and 1.5 µl of each primer (10 mM). The PCR program included DNA denaturation at 95 °C for 2 min, 25 cycles comprising DNA denaturation at 95 °C for 40 sec, hybridization at 58 °C for 40 sec and extension at 72 °C for 8 sec. PCR products were migrated by electrophoresis in a 1 % agarose gel in TAE 1X (TRIS-acetate 40 mM, EDTA 1 mM) for 2 h at 70 Volt and stained with BET (2 µg. mL-1).

2.3.6. Analysis of Strain Structuring

In order to examine the composition of the strains and establish the connections between them, we investigated classification and correlation characteristics. The two methods used were the Hierarchical Ascending Classification (HAC) and the correlation matrix (PCA). A dendrogram was used to illustrate the AHC. The parameters of interest included the collection years of the strains, their geographical origins, and their T3E repertoires.

2.4. Data Analysis

In order to analyze the outcomes, a reaction was deemed affirmative if a solitary distinct band of the anticipated size was observed on the agarose gel. Conversely, if no band was observed, the reaction was regarded as negative. The distribution was further categorized based on the presence or absence of the characterized effectors. The statistical analysis of the structured data and the representation of the graphs were conducted using the Minitab software 2018 and XLSTAT 2016 software packages.

3. Results

3.1. Strains Isolated

Based on the symptoms shown in Figure 2A, laboratory isolations showed strains with pale yellow colonies, circular in shape and mucous in appearance (Figure 2B).

(**A**) (**B**)

Figure 2. Citrus bacterial canker symptoms on *Citrus reticulata* × *Citrus paradisi* (A) and morphological appearance of isolated *Xcc* strains (B).

The pathogenicity test on the strains enabled us to observe symptoms characteristic of *Xcc* on *C. reticulata* × *C. paradisi*. This confirms that all the strains are pathogenic.

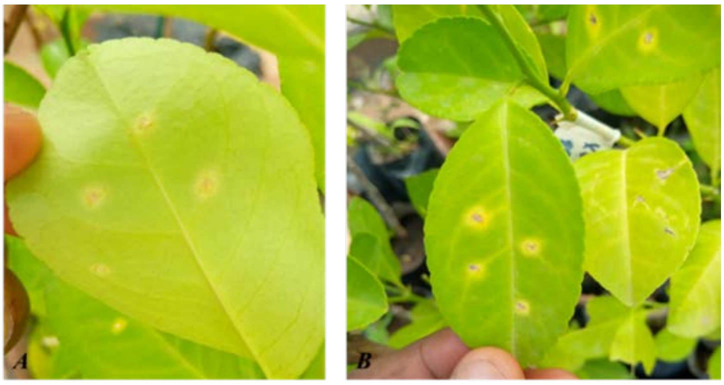

(**A**) (**B**)

Figure 3. Symptoms induced by *Xcc* strains after inoculation: Symptoms on the lower surface, (A) and Symptoms on the upper surface (B).

Through surveys conducted in citrus-growing regions of Burkina Faso between the periods of 2020 and 2021, a total of 17 strains were identified. Among them, 7 strains were isolated in 2020 and 10 strains were isolated in 2021. A total of twelve (12) strains were obtained from the cross between *C. reticulata* × *C. paradisi*, three (3) strains from *Citrus maxima*, and two (2) strains from *Citrus limon*. The majority of the strains that have been isolated originate from the Houet location. The limited number of strains utilized is associated with the significant challenges experienced during isolation, as well as the storage conditions that resulted in the loss of numerous strains.

Table 3. Characteristics of strains used.

Strain code	Hosts plants	Province	Site	Year of collection
80	*C. maxima*	Bazega	Timboué	2020
81	*C. limon*	Ziro	Lou	2020
82	*C. reticulata* × *C. paradisi*	Houet	Kodéni	2020
83	*C. reticulata* × *C. paradisi*	Kénédougou	Orodara	2020
84	*C. reticulata* × *C. paradisi*	Houet	Bobo Dioulasso	2020
85	*C. reticulata* × *C. paradisi*	Houet	Kodéni	2020
86	*C. reticulata* × *C. paradisi*	Houet	Bobo Dioulasso	2020
92	*C. maxima*	Bazega	Dayasmeré	2021
94	*C. reticulata* × *C. paradisi*	Houet	Kodéni	2021
95	*C. reticulata* × *C. paradisi*	Houet	Kodéni	2021
98	*C. reticulata* × *C. paradisi*	Ziro	Lou	2021
99	*C. maxima*	Bazega	Lilbouré	2021
100	*C. reticulata* × *C. paradisi*	Bazega	Lilbouré	2021
102	*C. reticulata* × *C. paradisi*	Houet	Bobo Dioulasso	2021
104	*C. limon*	Houet	Kodéni	2021
106	*C. reticulata* × *C. paradisi*	Houet	Bobo Dioulasso	2021
107	*C. reticulata* × *C. paradisi*	Ziro	Lou	2021

3.2. Distribution of Non-TAL Type 3 Effectors in Xcc Strains

The allocation of the 11 T3Es among the 48 *Xcc* strains is presented in table 4. In general, the strains that were isolated in 2020 and 2021 demonstrate a wider variety of T3E repertoires when compared to the strains from 2012. More precisely, the strains collected in 2012 did not possess the genes XopX, XopQ, XopD, XopO, and AvrBS1, whereas the strains recovered in 2020 and 2021 did have these genes. Furthermore, a total of 11 screened effectors were detected in three strains, specifically one strain from 2020 (Xcc85) and two strains from 2021 (Xcc102 and Xcc104). The distribution of Type 3 Effector Proteins (T3Es) across the strains identified in 2012 showed a virtually consistent and evenly spread pattern. The percentage distribution of T3Es suggests a prevalent occurrence of three effectors, specifically XopE2, XopN, and AvrBs2, across the strains. On the other hand, the effectors AvrBS1, XopO, and XopX are the least common, with frequencies of 16.4%, 16.7%, and 18.7% respectively.

Table 4. : Distribution of the 11 T3Es within *Xcc* strains.

Strains Code	**Type 3 effectors**										
	XopB	XopE2	XopN	XopX	XopQ	XopD	XopO	AvrxccA1	AvrxccA2	AvrBS1	AvrBS2
Strains isolated in 2020											
Xcc80	+	+	+	-	+	-	-	+	-	-	+
Xcc81	-	+	+	-	+	-	-	+	-	-	+
Xcc82	+	+	+	-	+	-	-	+	-	-	+
Xcc83	+	+	+	-	+	-	-	+	-	-	+
Xcc84	+	+	+	+	+	+	+	+	+	-	+
Xcc85	+	+	+	+	+	+	+	+	+	+	+
Xcc86	+	+	+	+	+	+	-	+	+	+	+
Strains isolated in 2021											
Xcc92	+	+	+	-	+	-	-	+	-	-	+
Xcc94	+	+	+	-		-	-	-	-	-	+
Xcc95	+	+	+	-	+	-	-	-	-	-	+
Xcc98	+	+	+	+	+	+	+	+	+	-	+

Xcc99	-	+	+	-	+	-	-	-	+	-	+
Xcc100	-	+	+	+	+	+	+	+	+	+	+
Xcc102	+	+	+	+	+	+	+	+	+	+	+
Xcc104	+	+	+	+	+	+	+	+	+	+	+
Xcc106	+	+	+	-	+	+	-	+	+	+	+
Xcc107	-	+	+	-	-	+	-	+	+	+	+
Strains isolated in 2022											
Xcc864	+	+	+	-	-	-	-	+	+	-	+
Xcc865	+	+	+	-	-	-	-	+	+	-	+
Xcc866	+	+	+	-	-	-	-	+	+	-	+
Xcc867	+	+	+	-	-	-	-	-	-	-	+
Xcc868	+	+	+	-	-	-	-	+	+	-	+
Xcc869	+	+	+	-	-	-	-	+	+	-	+
Xcc870	+	+	+	-	-	-	-	+	+	-	+
Xcc871	+	+	+	-	-	-	-	+	+	-	+
Xcc872	+	+	+	-	-	-	-	+	+	-	+
Xcc873	+	+	+	-	-	-	-	+	+	-	+
Xcc874	+	+	+	-	-	-	-	+	+	-	+
Xcc875	+	+	+	-	-	-	-	+	+	-	+
Xcc876	+	+	+	-	-	-	-	+	+	-	+
Xcc877	+	+	+	-	-	-	-	+	+	-	+
Xcc878	+	+	+	-	-	-	-	+	+	-	+
Xcc879	+	+	+	-	-	-	-	+	+	-	+
Xcc880	+	+	+	-	-	-	-	+	+	-	+
Xcc881	+	+	+	-	-	-	-	+	+	-	+
Xcc882	+	+	+	-	-	-	-	+	+	-	+

Xcc883	+	+	+	-	-	-	-	+	+	-	+
Xcc884	+	+	+	-	-	-	-	+	+	-	+
Xcc885	+	+	+	-	-	-	-	+	+	-	+
Xcc886	+	+	+	-	-	-	-	+	+	-	+
Xcc887	+	+	+	-	-	-	-	+	+	-	+
Xcc888	+	+	+	-	-	-	-	+	+	-	+
Xcc889	+	+	+	-	-	-	-	+	+	-	+
Xcc890	+	+	+	-	-	-	-	+	+	-	+
Xcc891	+	+	+	-	-	-	-	+	+	-	+
Xcc895	+	+	+	-	-	-	-	+	+	-	+
Xcc896	+	+	+	-	-	-	-	+	+	-	+
Xcc897	+	+	+	-	-	-	-	+	+	-	+
Attendance percentage (%)											
+	91,6	100	100	18,7	27,1	27,1	16,7	91,6	84,4	16,7	100

Note: In this table, the presence or the absence of an ortholog of each selected T3E gene was determined by hybridizations. **+** sign represent presence of the corresponding gene, whereas **-** sign represent absence of sequence similar to the probe used.

3.3. Geographical Distribution of T3Es

Figure 4 depicts the distribution of T3Es according to the geographical origins of the strains. The graph demonstrates that the Bobo-Dioulasso and Kodéni locations have the most variety, as all 11 screened T3Es were detected there. The Orodara and Lilbouré sites observed the existence of 10 T3Es, while the Timboué and Dayasmnaré sites had a lower diversity with five (05) T3Es. The Koloko, Tangoma, and Gnadga sites each recorded six (06) T3Es.

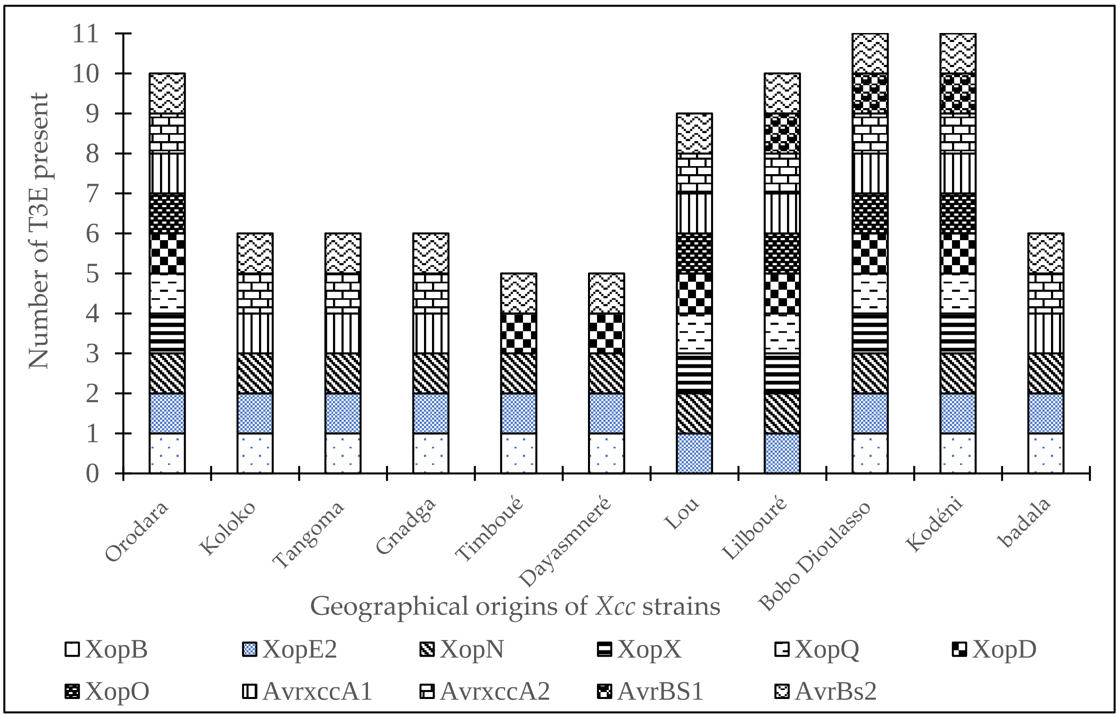

Figure 4. Distribution of E3T by localities.

Each color represents a T3E. The size of the diagram for each site depends on the number and the variability of T3E present

3.4. TALEs Diversity in Xcc Strains

An analysis of the distribution of TALEs among the *Xcc* strains shows the existence of two distinct patterns, referred to as Profile 1 and Profile 2. These patterns are characterized by different quantities of TALEs, ranging from two to three (Figure 5). Strains in Profile 1 include two TALEs (B and C), with TALE B amplified at a length of 2000 base pairs and TALE C somewhat longer than 2000 base pairs. In contrast, Profile 2 strains possess an extra TALE (A) in comparison to Profile 1 strains, and its amplification takes place at a length below 2000 bp.

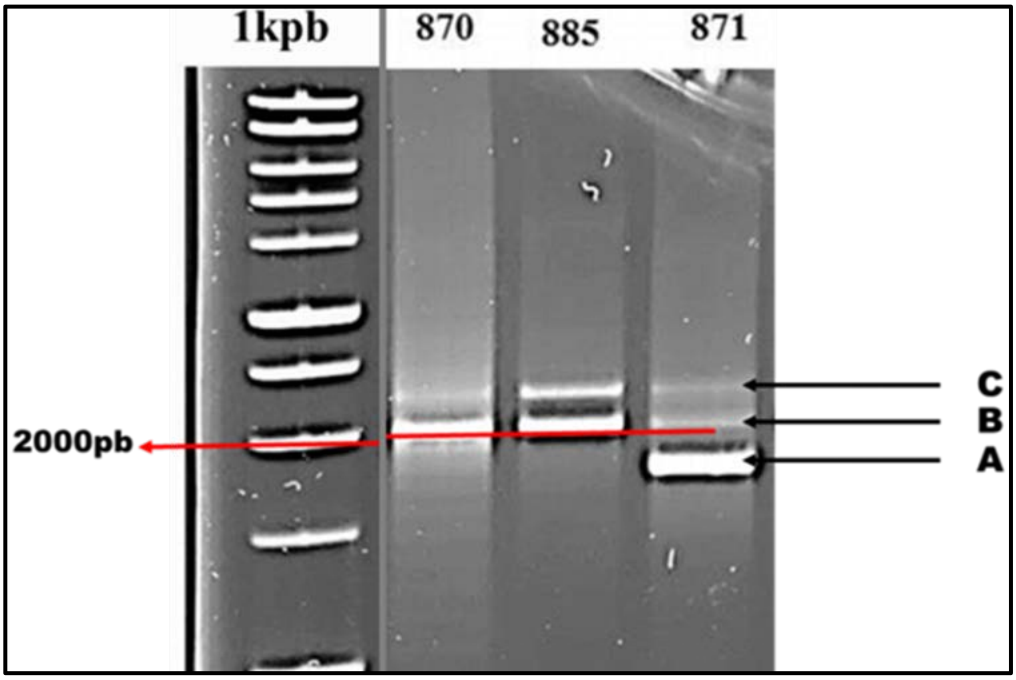

Figure 5. PCR detection of TALEs.

3.5. Distribution of TALEs by Strain

The examination of TALE distribution, as shown in table 4, reveals that TALEs B and C are found in all isolated *Xcc* strains, indicating a universal distribution with a prevalence of 100%. However, TALE A was found in 68.7% of the isolates. Profile analysis indicates that among the 48 examined *Xcc* strains, 37 strains demonstrate Profile 1, whereas the remaining 11 strains exhibit Profile 2. The strains acquired in 2020 include 11 Profile 2 strains, specifically Xcc80 and Xcc84. In 2021, two further strains, Xcc92 and Xcc102, were gathered. The remaining seven strains, namely Xcc871, Xcc879, Xcc881, Xcc882, Xcc887, Xcc896, and Xcc897, were collected in 2012.

Table 5. Distribution of TALEs by *Xcc* strain.

Years	Strains	TALE			Profil
		A	B	C	
2020	**Xcc80**	+	+	+	2
	Xcc81	-	+	+	1
	Xcc82	-	+	+	1
	Xcc83	-	+	+	1
	Xcc84	+	+	+	2
	Xcc85	-	+	+	1
	Xcc86	-	+	+	1
2021	**Xcc92**	+	+	+	2
	Xcc94	-	+	+	2
	Xcc95	-	+	+	1
	Xcc98	-	+	+	1
	Xcc99	-	+	+	1
	Xcc100	-	+	+	1
	Xcc102	+	+	+	1
	Xcc104	-	+	+	1
	Xcc106	-	+	+	1
	Xcc107	-	+	+	1
2012	**Xcc864**	-	+	+	1
	Xcc865	-	+	+	1
	Xcc866	-	+	+	1
	Xcc867	-	+	+	1
	Xcc868	-	+	+	1
	Xcc869	-	+	+	1
	Xcc870	-	+	+	1
	Xcc871	+	+	+	2
	Xcc872	-	+	+	1
	Xcc873	-	+	+	1
	Xcc874	-	+	+	1
	Xcc875	-	+	+	1
	Xcc876	-	+	+	1
	Xcc877	-	+	+	1
	Xcc878	-	+	+	1
	Xcc879	+	+	+	2
	Xcc880	-	+	+	1
	Xcc881	+	+	+	2
	Xcc882	+	+	+	2

Xcc883	-	+	+	1
Xcc884	-	+	+	1
Xcc885	-	+	+	1
Xcc886	-	+	+	1
Xcc887	+	+	+	2
Xcc888	-	+	+	1
Xcc889	-	+	+	1
Xcc890	-	+	+	1
Xcc891	-	+	+	1
Xcc895	-	+	+	1
Xcc896	+	+	+	2
Xcc897	+	+	+	2
Present (%)	68,7	100	100	

Note: In this table, the presence or the absence of an ortholog of each selected TALE gene was determined by hybridizations. **+** sign represent presence of the corresponding gene, whereas **-** sign represent absence of sequence similar to the probe used.

3.6. Hierarchical Ascending Classification

Strains were clustered using multivariate analysis, taking into account their geographical origin, TAL and non-TAL type 3 effector content, and year of separation. Based on these factors for each strain, a total of 12 separate groups were determined, as seen in the dendrogram displayed in Figure 5. The dendrogram allowed for the classification of all *Xcc* strains into 12 distinct categories. Strains obtained in 2012 were distributed over classes C5, C10, and C11, whereas strains from 2020 were primarily found in class C7. However, strains obtained in 2021 were evenly spread among the remaining classification categories. Out of the three strains that were isolated in 2020 and 2021 and tested with all TALEs, two of them (Xcc85 and Xcc104) were categorized as class C7. Strains containing three TALEs (Profile 2) that were obtained in 2012 were more prevalent in class C11, whereas the strains from 2012 (Xcc92 and Xcc94) were clustered together in class C4.

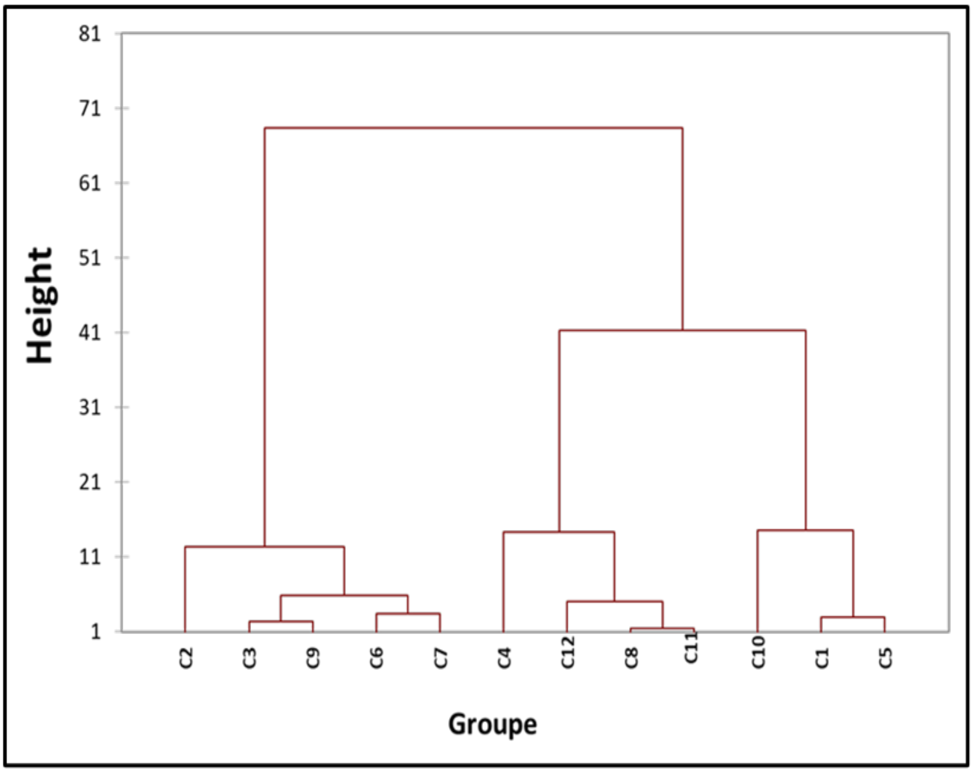

Figure 6. Hierarchical ascending classification.

C1 (876) ; C2 (84) ; C3 (102) ; C4 (92, 94, 106) ; C5 (888, 877, 878, 874, 875, 889) ; C6 (95) ; C7 (82, 85, 104, 98, 81, 83, 86, 107) ; C8 (897) ; C9 (99, 100) ; C10 (864, 865, 866, 867, 868, 869, 870, 872, 873, 880, 883, 884, 885, 886, 887, 890, 891, 895) ; C11 (871, 879, 881, 882, 896) ; C12 (80). Dissimilarity: Euclidean distance, aggregation method: Ward's method, interclass, percentage: 95 %.

3.7. Principal Component Analysis

Figure 7 displays the correlation matrix graphically representing the relationship between the geographical origin of the strains, the years they were isolated, and their TALE and T3E content. The analysis of variance revealed significant correlations among the different components, as evidenced by a p-value of less than 0.0001. An affirmative association was detected between the T3E repertoire and the duration of strain isolation. On the other hand, there was a negative link between the years when the strains were collected and their geographical origins. Significantly, there was no observed association between the TALE content of the strains and either their years of isolation or their geographical origins.

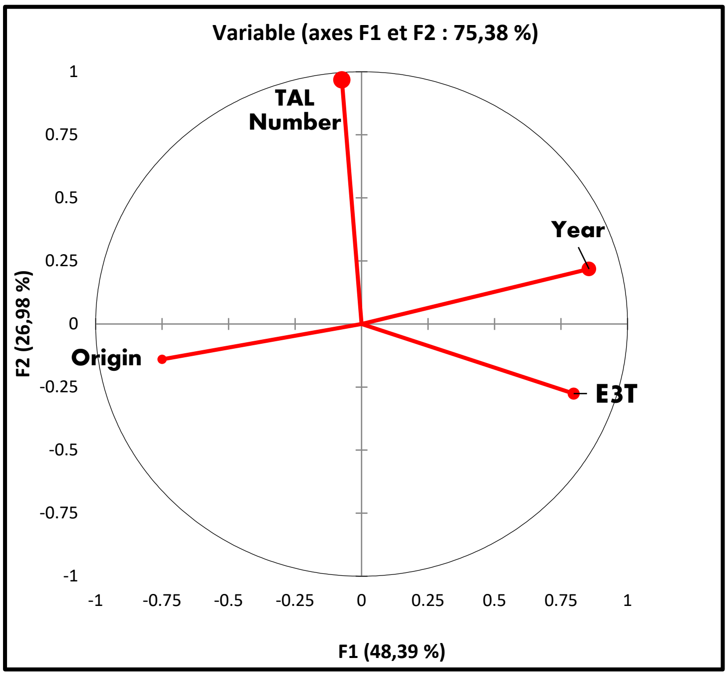

Figure 7. The degree of association between the distribution of T3E and the origin and year of collection of the strains.

4. Discussion

The analysis of T3E content in *Xcc* strains revealed the existence of genetic variations in T3E genes. More precisely, all *Xcc* strains included three T3E genes: XopE2, XopN, and AvrBs2. Strains that were obtained in 2020 and 2021 showed a common set of T3E (type III effector) genes and had higher variation in comparison to strains obtained in 2012. The persistent existence of these genes corresponds to the discoveries made in [15], indicating their participation in *Xcc* pathogenicity. The observed variations in T3E content between 2012 and subsequent years can be attributed to the ongoing cultivation of vulnerable varieties and the exchange of plant material within the country and neighboring regions like Mali and Côte d'Ivoire, which promotes the growth of more diverse and widespread *Xcc* populations.

Upon examination, it was shown that all *Xcc* strains examined included TALEs. Among the 48 strains that were tested, 11 of them possessed three TALEs, whereas the remaining 37 strains had two TALEs. This requirement of having at least two TALEs accords with the findings of reference [8]. Strains containing three TALEs, displaying traits of the A* pathotype, were detected, in line with recent findings from [13] that suggest the occurrence of the A* pathotype in Burkina Faso.

Nevertheless, the inadequate organization of T3E content according to geographical origin suggests a narrow range of strain variability, possibly because of the limited number of strains examined and the major focus on sampling from the Orodara locale, which is a crucial region for seedling production and distribution. Research conducted by [6] demonstrated that the majority of *Xcc* strains from Mauritius or Réunion were classified into specific groups known as RCCs, which were found in various locations across the island. The majority of the haplotypes from Grande Comore, Anjouan, and Mayotte exhibited a high degree of genetic similarity. The distribution of *Xcc* haplotypes within an island is typically limited to a single citrus block or to a nearby block. This indicates the dissemination of infected citrus plant material from commercial nurseries. The observed strain structuring may be influenced by diversification factors, such as environmental conditions. Lower variety in environmental parameters between collection locations may impede considerable strain evolution. The study demonstrated that strains coming from Mali and Burkina Faso exhibited a higher genetic similarity due to their close geographical proximity and nearly equal environmental circumstances between different zones. Nevertheless, our findings contradict the findings of [16], which demonstrated that the geographical location and close proximity of southern states, specifically Santa Catarina and Rio Grande do Sul, as well as neighboring countries where citrus canker is prevalent in South America (Argentina, Paraguay, and Uruguay), may have facilitated the transmission of infected plant material, resulting in the development of distinct populations of *Xcc*.

Examining the association between T3E distribution and the year of collection unveiled a positive connection, indicating a progression in strain distribution throughout time, regardless of geographical origin. This highlights several situations that influence the epidemiology and evolutionary dynamics of *Xcc* populations in Burkina Faso. Escalons' research indicates that the disease-causing ability of *Xcc* strains develops throughout time through a process of convergence within specific lineages. These data also demonstrate the dynamic nature of a pathogen's range of hosts [17].

5. Conclusions

The analysis of the T3E content of *Xcc* strains revealed that all examined strains shared a set of three identical T3E genes (XopE2, XopN, and AvrBs2). Nevertheless, there was noticeable variation in T3E levels among the strains isolated in 2020 and 2021, which is in contrast to the narrow range reported in strains from 2012. The analysis of TALEs revealed the existence of the 17.5-repeat TALE B in all strains that were examined. This particular TALE is a significant factor in the development of canker symptoms in pathotype A strains. The investigation also discovered two unique TALE profiles, with 11 strains classified under profile 2 and 37 strains classified under profile 1. The geographical origin of strains did not have a significant influence on their distribution. However, there was a clear positive relationship between the content of T3E (type III effector) and the number of years the strains had been isolated. This indicates that strains are distributed independently across different geographical locations and provides insights into the evolutionary dynamics of *Xcc* populations in Burkina Faso.

Author Contributions: Conceptualization, I.W. and K.B.F.Z.; methodology, K.B.F.Z. and FY; software, K.B.F.Z. and FY; formal analysis, K.B.F.Z; writing original draft preparation, K.B.F.Z. and FY., supervision, I.W. and I.S All authors have read and agreed to the published version of the manuscript.

Funding: This research received no external funding.

Institutional Review Board Statement: Not Applicable.

Informed Consent Statement: Not Applicable.

Data Availability Statement: The original data presented in the study are included in the article,. further inquiries can be directed to the corresponding author.

Acknowledgments: The authors would like to thank the phytopathology/bacteriology laboratory of INERA Farako-Bâ, Bobo Dioulasso (Burkina Faso), LMI PathoBios, France, and the plant clinic of NAZI Boni University, Bobo Dioulasso (Burkina Faso).

Conflicts of Interest: The authors declare no conflict so interest.

References

1. Ference, C. M.; Gochez, A. M.; Behlau, F.; Wang, N.; Graham, J. H.; Jones, J. B. Recent advances in the understanding of *Xanthomonas citri* ssp. *citri* pathogenesis and citrus canker disease management. *Mol. Plant Pathol.* **2018**, *19* (6), 1302–1318. https://doi.org/10.1111/mpp.12638.
2. Wang, N. The citrus hanglongbing crisis and potential solutions. *Mol. Plant* **2019**, *12* (5), 607–609. https://doi.org/10.1016/j.molp.2019.03.008.
3. Juhasz, C. C.; Leduc, A.; Boyer, C.; Guérin, F.; Vernière, C.; Pruvost, O.; Wonni, I.; Ouedraogo, L. First report of *Xanthomonas citri* pv. *citri* Causing Asiatic Citrus Canker in Burkina Faso. *Plant Dis.* **2013**, *97* (12), 1653–1653. https://doi.org/10.1094/PDIS-06-13-0600-PDN.
4. Zerbo, K. B. F.; Wonni I.; Yameogo F.; Somda, I., Antibacterial activity of some substances against citrus bacterial canker caused by *Xanthomonas citri* pv. *citri* (Hasse) in Burkina Faso. *Afr. J. Plant Sci.* **2022**, *16* (6), 138–147.
5. Young, J. M.; Park, D.-C.; Shearman, H. M.; Fargier, E. A Multilocus Sequence Analysis of the Genus Xanthomonas. *Syst. Appl. Microbiol.* **2008**, *31* (5), 366–377. https://doi.org/10.1016/j.syapm.2008.06.004.
6. Pruvost, O.; Richard, D.; Boyer, K.; Javegny, S.; Boyer, C.; Chiroleu, F.; Grygiel, P.; Parvedy, E.; Robène, I.; Maillot-Lebon, V.; Hamza, A.; Lobin, K. K.; Naiken, M.; Vernière, C. Diversity and geographical structure of *Xanthomonas citri* pv. *citri* on Citrus in the South West Indian Ocean Region. *Microorganisms* **2021**, *9* (5), 945. https://doi.org/10.3390/microorganisms9050945.
7. Bui Thi Ngoc, L.; VerniÃ¨re, C.; Belasque, J.; Vital, K.; Boutry, S.; Gagnevin, L.; Pruvost, O. Ligation-Mediated PCR, a fast and reliable technique for insertion sequence-based typing of *Xanthomonas citri* pv. *citri*. *FEMS Microbiol. Lett.* **2008**, *288* (1), 33–39. https://doi.org/10.1111/j.1574-6968.2008.01331.x.
8. Aline Escalon. Evolution et spécialisation du pouvoir pathogène de *Xanthomonas citri* pv. *citri* : Rôle des effecteurs de Type 3. *Agritop* **2013**, 258.
9. Kay, S.; Hahn, S.; Marois, E.; Wieduwild, R.; Bonas, U. Detailed analysis of the DNA recognition motifs of the *Xanthomonas* Type III Effectors AvrBs3 and AvrBs3Δrep16. *Plant J.* **2009**, *59* (6), 859–871. https://doi.org/10.1111/j.1365-313X.2009.03922.x.
10. Da Silva, A. C. R.; Ferro, J. A.; Reinach, F. C.; Farah, C. S.; Furlan, L. R.; Quaggio, R. B.; Monteiro-Vitorello, C. B.; Sluys, M. A. V.; Almeida, N. F.; Alves, L. M. C.; Do Amaral, A. M.; Bertolini, M. C.; Camargo, L. E. A.; Camarotte, G.; Cannavan, F.; Cardozo, J.; Chambergo, F.; Ciapina, L. P.; Cicarelli, R. M. B.; Coutinho, L. L.; Cursino-Santos, J. R.; El-Dorry, H.; Faria, J. B.; Ferreira, A. J. S.; Ferreira, R. C. C.; Ferro, M. I. T.; Formighieri, E. F.; Franco, M. C.; Greggio, C. C.; Gruber, A.; Katsuyama, A. M.; Kishi, L. T.; Leite, R. P.; Lemos, E. G. M.; Lemos, M. V. F.; Locali, E. C.; Machado, M. A.; Madeira, A. M. B. N.; Martinez-Rossi, N. M.; Martins, E. C.; Meidanis, J.; Menck, C. F. M.; Miyaki, C. Y.; Moon, D. H.; Moreira, L. M.; Novo, M. T. M.; Okura, V. K.; Oliveira, M. C.; Oliveira, V. R.; Pereira, H. A.; Rossi, A.; Sena, J. A. D.; Silva, C.; De Souza, R. F.; Spinola, L. A. F.; Takita, M. A.; Tamura, R. E.; Teixeira, E. C.; Tezza, R. I. D.; Trindade Dos Santos, M.; Truffi, D.; Tsai, S. M.; White, F. F.; Setubal, J. C.; Kitajima, J. P. Comparison of the genomes of two Xanthomonas pathogens with differing host specificities. *Nature* **2002**, *417* (6887), 459–463. https://doi.org/10.1038/417459a.
11. Castiblanco, L. F.; Gil, J.; Rojas, A.; Osorio, D.; Gutiérrez, S.; Muñoz-Bodnar, A.; Perez-Quintero, A. L.; Koebnik, R.; Szurek, B.; López, C.; Restrepo, S.; Verdier, V.; Bernal, A. J. TALE 1 from *Xanthomonas axonopodis* pv. *manihotis* acts as a Transcriptional Activator in plant cells and is important for pathogenicity in cassava Plants. *Mol. Plant Pathol.* **2013**, *14* (1), 84–95. https://doi.org/10.1111/j.1364-3703.2012.00830.x.
12. Boch, J.; Bonas, U.; Lahaye, T. TAL Effectors – pathogen strategies and plant resistance engineering. *New Phytol.* **2014**, *204* (4), 823–832. https://doi.org/10.1111/nph.13015.
13. Leduc, A.; Traoré, Y. N.; Boyer, K.; Magne, M.; Grygiel, P.; Juhasz, C. C.; Boyer, C.; Guerin, F.; Wonni, I.; Ouedraogo, L.; Vernière, C.; Ravigné, V.; Pruvost, O. Bridgehead invasion of a monomorphic plant pathogenic bacterium: *Xanthomonas citri* pv. *citri* , an emerging citrus pathogen in Mali and Burkina Faso. *Environ. Microbiol.* **2015**, *17* (11), 4429–4442. https://doi.org/10.1111/1462-2920.12876.
14. Hajri, A.; Pothier, J. F.; Fischer-Le Saux, M.; Bonneau, S.; Poussier, S.; Boureau, T.; Duffy, B.; Manceau, C. Type three effector gene distribution and sequence analysis provide new insights into the pathogenicity of plant-pathogenic *Xanthomonas arboricola*. *Appl. Environ. Microbiol.* 2012, *78* (2), 371–384. https://doi.org/10.1128/AEM.06119-11.
15. Escalon, A.; Javegny, S.; Vernière, C.; Noël, L. D.; Vital, K.; Poussier, S.; Hajri, A.; Boureau, T.; Pruvost, O.; Arlat, M.; Gagnevin, L. Variations in Type III Effector repertoires, pthological phenotypes and host range of *Xanthomonas citri* pv. *citri* pathotypes. *Mol. Plant Pathol.* 2013, *14* (5), 483–496. https://doi.org/10.1111/mpp.12019.

16. Jaciani, F. J.; Ferro, J. A.; Ferro, M. I. T.; Vernière, C.; Pruvost, O.; Belasque, J. Genetic Diversity of a Brazilian strain collection of *Xanthomonas citri* subsp. *citri* based on the Type III Effector Protein Genes. *Plant Dis.* **2012**, *96* (2), 193–203. https://doi.org/10.1094/PDIS-04-11-0357.
17. Schulze-Lefert, P.; Panstruga, R. A Molecular evolutionary concept connecting nonhost resistance, pathogen host range, and pathogen speciation. *Trends Plant Sci.* **2011**, *16* (3), 117–125. https://doi.org/10.1016/j.tplants.2011.01.001.